Physics Letters B 665 (2008) 152–156

Contents lists available at ScienceDirect

Physics Letters B

www.elsevier.com/locate/physletb

Challenging nuclear structure models through a microscopic description of proton inelastic scattering off ^{208}Pb

M. Dupuis [a,1], S. Karataglidis [a,2], E. Bauge [a,*], J.-P. Delaroche [a], D. Gogny [b]

[a] Commissariat à l'Energie Atomique, Centre DAM—Ile de France, Service de Physique Nucléaire, Bruyères-le-Châtel, 91297 Arpajon CEDEX, France
[b] L-414, Lawrence Livermore National Laboratory, Livermore, CA 94551, USA

ARTICLE INFO

Article history:
Received 5 March 2008
Received in revised form 7 May 2008
Accepted 15 May 2008
Available online 5 June 2008
Editor: J.-P. Blaizot

PACS:
21.60.Jz
24.10.Ht
24.10.Eq

ABSTRACT

Differential cross sections from fully microscopic calculations of inelastic proton scattering off ^{208}Pb are compared to experimental scattering data for incident proton energies between 65 and 201 MeV. The required nucleon–nucleus interactions were formed by folding nuclear structure information with a reliable nucleon–nucleon effective interaction that has no adjustable parameter. The absence of phenomenological normalisation in our approach offers the possibility to interpret with confidence the calculated results in terms of the quality of the underlying nuclear structure description: a feature that had been reserved, until recently, to the electron probe. We have used this method to investigate the effect of long range correlations embedded in excited states on calculated inelastic observables and demonstrate the sensitivity of nucleon scattering predictions to details of the nuclear structure.

In the past, the structure of ground and excited states of stable nuclei has been probed extensively with high energy electron scattering experiments. Since the Coulomb interaction and its treatment in a scattering problem are both well known, ground state charge and transition densities can be extracted from scattering observables accurately and in a model-independent way. As well, analyses of elastic and inelastic data from proton scattering have been used to assess nuclear structure and descriptions of the in-medium nucleon–nucleon (*NN*) interaction. But disentangling structure effects from those due to the in-medium nuclear interaction is not as easy, or unambiguous, as in the case of the electron probe.

Proton inelastic scattering from heavy nuclei already has been modelled within several frameworks besides that which we adopt. But each of those other approaches involves either some phenomenological adjustment for the nucleon–nucleus (*NA*) interaction, simplification to the nuclear structure details, or relies on approximations whose effects are not well controlled. The earliest of these used the phenomenological collective model in a Born approximation. From those analyses, assignments of spin-parities to numerous excitations were made. More recently, inelastic scattering data were analysed [1] using microscopic transition densities from quasi-particle random phase approximation (QRPA) calculations within a distorted wave approximation (DWA). However, the associated evaluations involve several renormalisation processes, both for the *NA* interactions and for the QRPA transition densities. As well, an approximate treatment of the exchange transition amplitudes often was used. Hence those analyses of proton scattering data do not seriously challenge specifics of nuclear structure since any observed agreement cannot be assigned unambiguously to either effects of the adjustments/approximations or to the intrinsic quality of the underlying nuclear structure model itself.

Recent progress in the understanding of nuclear interactions now permits precise analyses of nucleon scattering data to be tests of the quality of structure information with much less ambiguity. For example, the Melbourne *g*-matrix, an in-medium *NN* interaction [2], has been used successfully in microscopic model calculations of elastic and inelastic *NA* scattering. When used with accurate structure information, the method predicted scattering observables in very good agreement with experimental data. In particular, that approach lead to excellent agreement with data from the elastic scattering of 65 and 201 MeV protons over a wide range of masses of the target [2–5] including exotic nuclei [3,6,7]. For elastic scattering, the process has been termed *g*-folding which signifies that the in-medium *NN* interaction is folded with the structure wave functions forming a non-local optical potential as the *NA* interaction [2]. Similar agreement has also been achieved in describing, self-consistently, inelastic scattering off light-mass nuclei (^{12}C, ^{14}N, ^{16}O) [6,8], i.e. when the same effective *g*-matrix was used for the transition operators and for the *g*-folding *NA* potential from which the distorted waves to be used in a DWA calculation were generated. The accurate predictions (no adjustable parameters) so found, of the differential cross sections and analysing

* Corresponding author.
E-mail address: eric.bauge@cea.fr (E. Bauge).
[1] Present address: Los Alamos National Laboratory, Los Alamos, NM, USA.
[2] Present address: Department of Physics and Electronics, Rhodes University, Grahamstown 6140, South Africa.

0370-2693 © 2008 Elsevier B.V. Open access under CC BY license.
doi:10.1016/j.physletb.2008.05.061

powers from elastic and inelastic scattering for both natural parity and unnatural parity transitions, demonstrate that all components of the in-medium *NN* interaction (central, spin–orbit and tensor) are realistic. From those analyses, valuable information about nuclear excited states, such as particle–hole decomposition [9] and the degree of isospin mixing of some excitations [8] could be specified, and the Gamow–Teller strength for double beta decay assessed [10].

In the present work, this method of making fully microscopic analyses of proton scattering data has been used with data from inelastic proton scattering off heavy spherical nuclei for which mean-field and beyond the mean-field calculations are preferred to the shell-model approaches previously used for lighter-mass nuclei. Specifically, calculations of proton inelastic scattering off ^{208}Pb have been made. The structure information required has been obtained from Self-Consistent RPA (SCRPA) calculations [11]. In the present context, Self-Consistency means that the same interaction (the D1S interaction [12]) is used for calculating the mean field single particle states, and as the residual interaction in RPA calculations. The present work is a natural extension of our previous study of proton elastic scattering [13] since in that we used the same structure information and the same microscopic effective interactions. Therein [13] it was shown that the SCRPA + D1S description of the structure of doubly closed shell nuclei accounts comparably well for the elastic scattering of both electrons and medium energy protons.

In this Letter, first we demonstrate that it is possible to describe inelastic proton scattering off doubly-closed shell heavy nuclei in a fully-microscopic framework with the same accuracy as that which has been obtained for scattering off light-mass nuclei. For this purpose, predictions of differential inelastic cross sections for many excited states of ^{208}Pb with incident proton energy between 65 and 201 MeV will be discussed. Those calculations were performed within a single microscopic framework, with the same *NA* interaction and the same structure model for all transitions. No normalisation process was involved and the knock-on exchange amplitudes were treated exactly. Even though that structure framework has already been tested by comparison of theoretical with experimental charge transition densities [22], proton inelastic scattering calculations are complementary tests since they are sensitive to both proton and neutron components of the RPA transition densities. Further, the dominance of the isoscalar $^3S_1$ component of the *NN* interaction [2] ensures that proton scattering observables are particularly sensitive to the neutron transition densities; something that is not significantly probed with studies of electron scattering.

Our second motivation was to show that a relevant conclusion on nuclear structure can only be obtained from calculations of proton scattering observables if those evaluations are very accurate and involve no adjustment process. For this purpose, we compare results from our proton inelastic scattering calculations for high spin excitations to previous ones found using a semi-phenomenological scattering model. Those semi-phenomenological model results lead to some contradictory conclusions about the properties of the states. The scatterings to the high spin states have also been used to assess the effect of "degraded" descriptions of the structure on proton scattering observables. By that means the sensitivity of the scattering observables to details of the nuclear structure of the target is revealed. Finally, it is worth mentioning the current experimental effort to provide accurate proton inelastic scattering data on exotic nuclei. The derivation of a predictive microscopic approach, such as the one we propose, could be a very powerful tool to analyse and interpret these data [14].

For the inelastic scattering of a nucleon off a zero-spin ground state, the differential cross sections have been calculated from the DWA expression of the transition amplitude,

$$\mathcal{T}_{fi}(\Omega_{sc}) = \big\langle \chi^-(\mathbf{k}_f), n \big| V_{\rm eff} \big| \chi^+(\mathbf{k}_i), \tilde{0} \big\rangle, \tag{1}$$

associated with excitations $|n\rangle$ of the target originally in the ground state $|\tilde{0}\rangle$. The incoming $\chi^+(\mathbf{k}_i)$ and outgoing $\chi^-(\mathbf{k}_f)$ distorted waves in Eq. (1) were obtained by solving the one-body Schrödinger equation describing the elastic scattering of a nucleon from the nucleus. That involved the non-local, g-folding optical potentials formed using the target state structure described within the SCRPA + D1S framework for double-closed shell nuclei [13]. Full details of the folding procedure may be found in [2]. For more information on the definition and the characteristics of the optical potential we refer also the readers to the report by Jeukenne et al. [15]. As was done previously [13], the true RPA correlated ground state $|\tilde{0}\rangle$, which includes corrections for the quasi-boson approximation, was used. We have not used the uncorrelated Hartree–Fock ground state. The effective interaction used in the g-folding is the Melbourne g-matrix (solution of the relevant Brueckner–Bethe–Goldstone equations [2]) which includes central, tensor and spin–orbit components that are complex, energy and density dependent. The optical potential so formed is then complex and energy dependent. The $V_{\rm eff}$ interaction generating the transition in Eq. (1) is also the Melbourne g-matrix. Excited states $|n\rangle = |N J \Pi M\rangle$ of multipolarity, parity J, Π and spin projection M are then written as RPA excitations of $|\tilde{0}\rangle$,

$$\begin{aligned} |n\rangle = |N J \Pi M\rangle &= \Theta^+_{N J \Pi M} |\tilde{0}\rangle \\ &= \sum_{ph\in(J\Pi)} \big[X^N_{ph} A^+_{JM\Pi}(p\tilde{h}) - Y^N_{ph} A_{J\bar{M}\Pi}(p\tilde{h}) \big] |\tilde{0}\rangle. \end{aligned} \tag{2}$$

The different quantities and operators appearing in this equation are defined in Ref. [13]. The X and Y amplitudes were obtained by solving the RPA equations for which the particle–hole interaction has been used in a self-consistent way, i.e. it has been derived from the second derivative of the energy density functional obtained with the D1S interaction.

The structure information that enters the DWA matrix elements is the one-body-density-matrix elements (OBDMEs) since the fully antisymmetric formulation of the transition amplitudes involves local and non-local components. Hereafter termed density matrices or OBDMEs, the general expression of these elements is

$$\begin{aligned} &\rho^n_{\pm\frac{1}{2},\pm\frac{1}{2}}(\mathbf{r},\mathbf{r}',\boldsymbol{\sigma},\boldsymbol{\sigma}') \\ &\quad = \sum_{\alpha,\beta} \langle n | b^+_{\alpha,\pm\frac{1}{2}} b_{\beta,\pm\frac{1}{2}} |\tilde{0}\rangle \phi^*_\alpha(\mathbf{r}) \chi^{\frac{1}{2}\ *}_{\pm\frac{1}{2}}(\boldsymbol{\sigma}) \phi_\beta(\mathbf{r}') \chi^{\frac{1}{2}}_{\pm\frac{1}{2}}(\boldsymbol{\sigma}'), \end{aligned} \tag{3}$$

where $\alpha \equiv (n_\alpha, l_\alpha, m_\alpha)$, $\phi_\alpha(\mathbf{r}) = \langle \mathbf{r} | n_\alpha l_\alpha m_\alpha \rangle$ and $\chi^{\frac{1}{2}}_{\pm\frac{1}{2}}(\boldsymbol{\sigma}) = \langle \boldsymbol{\sigma} | \frac{1}{2}, \pm\frac{1}{2} \rangle$. The quantum numbers set $\alpha, \pm\frac{1}{2}$ refers to a Hartree–Fock single particle state for which the intrinsic spin and the angular momentum are uncoupled. Since we do not consider charge exchange reactions, we discard any dependence on the isotopic spin. The $\mathbf{r} = \mathbf{r}'$ case summed over the spin projections corresponds to the matter transition density which after angular integration has the form

$$\rho^n(r) = \sum_{ph\in(J\Pi)} \big(X^N_{ph} + Y^N_{ph} \big) \phi^*_p(r) \phi_h(r) C(j_p, j_h, J, L_p, l_h), \tag{4}$$

where $C(j_p, j_h, J, L_p, l_h)$ is a simple geometric factor (see Ref. [11] for more details). Transition densities such as these have been used solely as the structure input in previous DWA evaluations, but it is now well established [2–9] that the full OBDMEs are essential in evaluations of both elastic and inelastic, medium-energy, *NA* scattering.

We present differential cross sections calculated with the method described above, namely with the Melbourne g-matrix

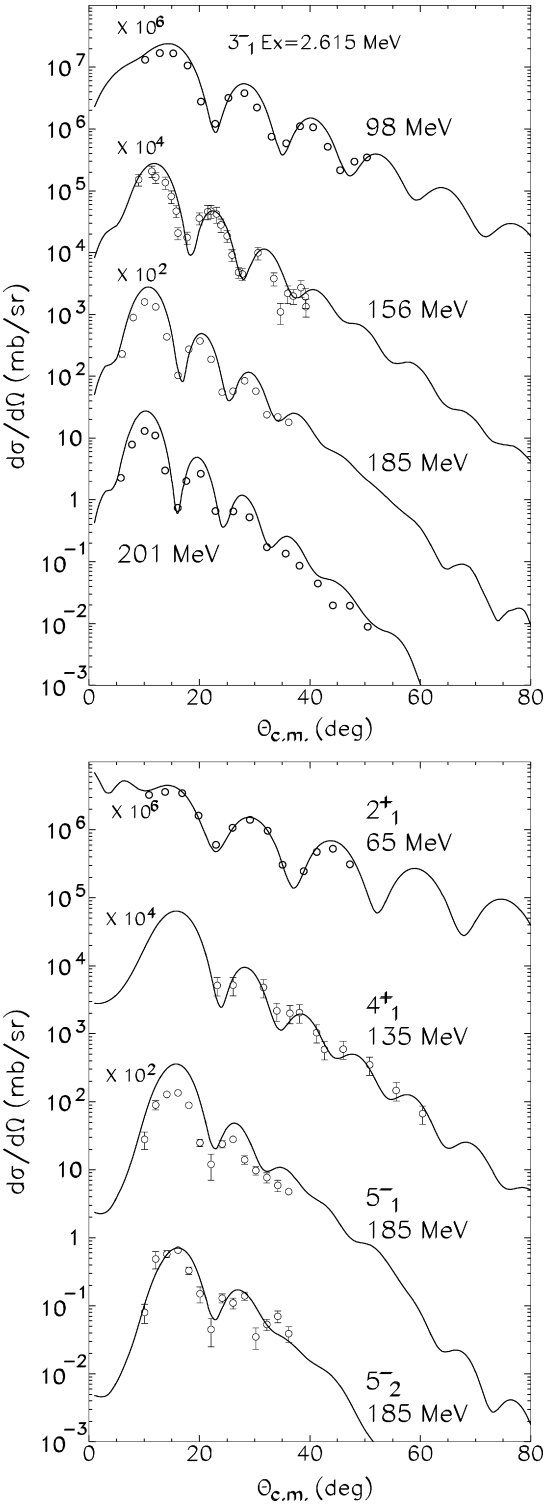

Fig. 1. Proton inelastic scattering leading to the 3^-_1 (2.615 MeV), 2^+_1 (4.085 MeV), 4^+_1 (4.323 MeV), 5^-_1 (3.197 MeV), and 5^-_2 (3.708 MeV) excited states of ^{208}Pb. The incident energies are indicated on the plot. The results of the Melbourne + SCRPA + D1S model cross sections are displayed by solid curves. The open circles are the experimental data [16–21].

folded with the SCRPA + D1S description of ground and excited states. Comparisons between our calculations and experimental data [16–21] are shown in Fig. 1 for inelastic scattering of protons. Cases for diverse incident energies in the range 65 to 201 MeV leading to the 3^-_1, 2^+_1, 4^+_1, 5^-_1 and 5^-_2 excited states of ^{208}Pb are displayed. The overall agreement between theoretical calculations and data is very good. For the 3^-_1 excited state, cross sections are shown at four proton incident energies between 98 and 201 MeV, and our calculated results agree very well with the experimental data, in shape and in magnitude. Such is indicative of the quality of the Melbourne g-matrix (including its energy dependence) as well as the underlying SCRPA description of the 3^-_1 state. Good agreement (Fig. 1) between evaluated cross sections and data also is evident for the 2^+_1, 4^+_1 and 5^-_2 state excitations at the select single incident energy in each case. Note that experimental data are available for these states at other incident energies. In this Letter, we only display a representative sample of our calculations. An exhaustive comparison to all available data, which are as well described by our model, is postponed to a future paper. In the present analysis, the only exception to the overall good agreement is the transition to the 5^-_1 state for which the calculated cross-section magnitude at the forward angle peak is twice stronger than the experimental one. We also notice a slight overestimation for the transition to the 3^-_1 state. We remind that the dominance of the proton–neutron interaction makes proton scattering observables particularly sensitive to the neutron component of the transition density. Thus, our analysis clearly reveals an overestimation of the calculated neutron transition densities associated to these two excitations. Discrepancies of the same magnitude are also observed in analyses of electron scattering cross sections [22], which reveal that the proton transition densities calculated with the SCRPA + D1 are also overestimated (the results obtained with the D1S interaction are quasi-identical). Note that an unique renormalisation factor of the total transition density would lead to a good agreement between theoretical predictions and experiments for proton and electron scattering. Yet, our proton scattering analysis complements the observations made from electron scattering data analyses as it reveals an equivalent deficiency in both the proton and neutron components of the transition density.

The same SCRPA + D1S transition densities were used previously [23], within a semi-phenomenological model, to calculate high energy proton inelastic scattering leading to some discrete states of ^{208}Pb. The cross sections obtained in that study needed sizable renormalisation factors to account for the data which lead the authors to claim that the structure information was inaccurate. However, our results disagree with this conclusion and confirm the relevance of the SCRPA + D1S density matrices for use in inelastic scattering calculations when a better reaction model is considered.

In Fig. 2, we compare experimental inelastic differential cross sections [24] and our calculated ones for transitions to high spin states, namely to the 8^+_1, 10^+_1 and 12^+_1 states. The solid lines are the results of calculations performed with the Melbourne g-matrix folded with the SCRPA + D1S transition density matrices. Even for these high spin states, the comparisons are excellent. Again, note that our calculations involve no normalisation process. Of relevance here is that these high spin states have a correlated structure that must be described very accurately. First, the description of the 8^+_1 state not only involves ~ 440 particle–hole pairs but it also contains collectivity that is reflected in the RPA description by "large" Y components. These facets must not be ignored in scattering calculations. The collectivity is illustrated in Fig. 2 with the result of a calculation made omitting the Y components (dotted curve) which lies 30% below the complete calculation result (full curve). An example of the nuclear structure accuracy needed for nucleon scattering calculations is given by the result obtained when seemingly minor particle–hole components are neglected. The dashed and dotted-dashed curves for the 8^+_1 transition correspond to the calculations which neglect configurations for which $Z < 0.01$ and $Z < 0.1$, respectively, with $Z = X$ and/or Y. Given the normalisation of states,

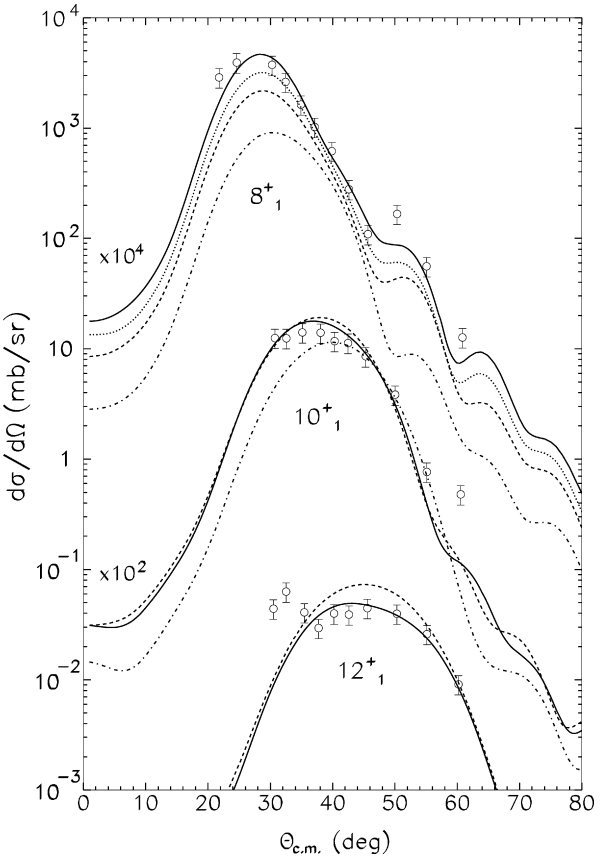

Fig. 2. Proton inelastic scattering off the 8^+_1 (4.610 MeV) 10^+_1 (4.895 MeV) and 12^+_1 (6.097 MeV) excited states of ^{208}Pb at 135.2 MeV. Experimental data are from [18]. The results of the Melbourne + SCRPA + D1S model calculations are displayed as solid curves, the other curves are defined in the text.

$$N^2 = \langle n|n\rangle = \sum_{ph\in(J\Pi)} \left[\left(X^N_{ph}\right)^2 - \left(Y^N_{ph}\right)^2\right] = 1, \tag{5}$$

these two truncations would seem to be good approximations since they correspond to a norm of $N^2 = 0.957$, with 4 particle–hole components ($Z > 0.1$), and a norm of $N^2 = 0.999$ with 39 particle–hole components ($Z > 0.01$). Yet, the effect of these truncations on the inelastic scattering cross sections is striking. Indeed, for the second truncation ($N^2 = 0.999$), the calculated cross section lies 50% below the complete result and for the first truncation ($N^2 = 0.957$), the calculated cross section is five times lower than for the complete result. Furthermore the shape of the cross sections changes under these truncations in structure.

The results for the excitations of the 10^+_1 and 12^+_1 states are discussed later, for at this point, it is useful to consider the impact of truncations on the local proton and neutron transition densities associated with the 8^+_1 state. They are shown in Fig. 3. The four sets of transition densities associated with the four cross-section results reveal that the different truncations of the configuration space of the RPA components (cancelled Y components or Z limited to components larger than 0.1 or 0.01) are clearly reflected in neutron and, to a lesser extent, proton transition densities. Although our proton scattering calculations involve the full non-local transition and current densities, the local densities shown in Fig. 3 can still help to interpret the results of proton scattering calculations with different configuration space truncations. Indeed, the differences between proton inelastic scattering calculations of the 8^+_1 state excitation qualitatively track the changes of the associated neutron transition densities, as expected with a dominant $^3S_1$ NN interaction component in the NN g-matrix. This highlights the

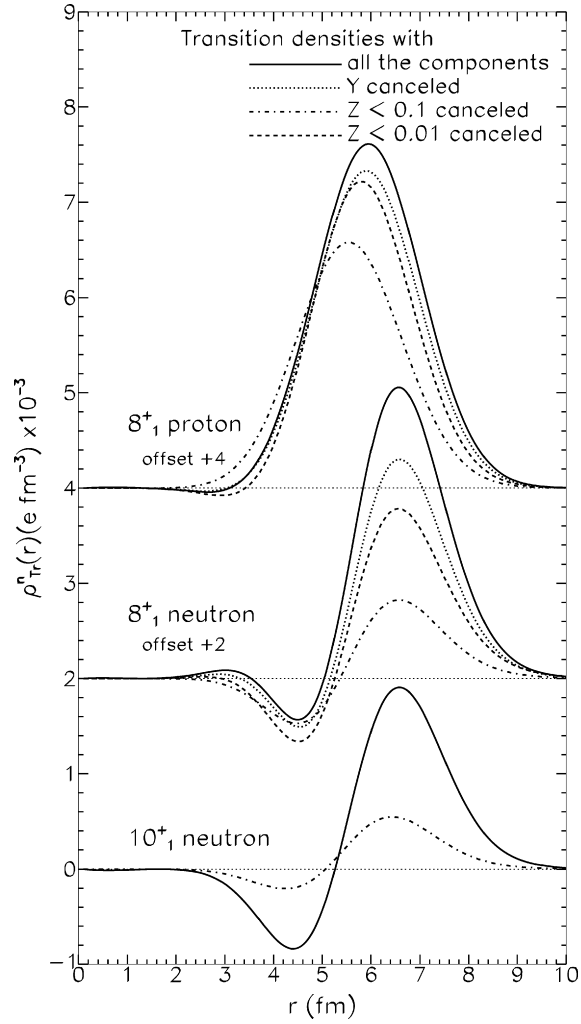

Fig. 3. Proton and neutron local transition densities to the 8^+_1 and 10^+_1 states calculated within the SCRPA + D1S framework with different truncations of configuration space.

effect of the long range correlation included in the SCRPA + D1S structure model. Those correlations manifest in seemingly minor Z components which nevertheless work coherently to produce strong effects in either local transition densities and/or in our inelastic proton scattering cross sections. Since, for the transition under consideration, the contribution to the proton scattering comes mainly from the neutron component of the transition density it is difficult to extract precise information on the structure of the proton component. In this case, both proton and electron scattering observables are necessary to test the full transition density.

Returning to the cross sections displayed in Fig. 2, those for the transition to the 10^+_1 state exhibit similar behaviour to that seen for the excitation of the 8^+_1 state. The 10^+_1 excited state presents weaker collectivity, but 39 particle–hole components are still needed to accurately describe inelastic scattering. That contrasts with previous analyses [25] where this state was described with only three or four particle–hole configurations. In Fig. 2, for the 10^+_1 case, the dashed line is the result of a calculation for which the Z components lower than 0.1 have been omitted. Then only three particle–hole components remain but the norm $N^2 = 0.984$ is still close to one. However the effect on calculated cross sections is sizable since the "truncated" calculation result is 30% below the complete one and the cross section maximum is also shifted by 4 degrees. As seen in Fig. 3, the relevant neutron local transition densities change in a way that is qualitatively

consistent with the results of our proton inelastic scattering calculations. Truncating the configuration space produced almost no effect on the proton transition densities in this case.

The transition to the 12_1^+ state is well-described by the single-particle–hole configuration $\nu(i_{9/2}, i_{13/2}^{-1})$. In Fig. 2, we compare results of the calculation made with the Melbourne g-matrix (full curve) with that found using the M3Y interaction [26] (dashed curve). Such also has been done for the transition to the 10_1^+ state. For the 10_1^+ transition, the result of the calculation performed with the M3Y interaction is very close to that obtained with the Melbourne g-matrix. But for the 12_1^+ transition, the two evaluations give distinctly different cross sections. Using the M3Y interaction produced an inelastic scattering cross section $\sim 25\%$ larger than the data; a result also obtained in a previous analysis using that interaction [25]. To explain that over-prediction, a quenching effect for this particle–hole excitation was postulated [25]. However, using the Melbourne g-matrix with the same structure information, the data is well matched and there is no need for any quenching. This is a clear example for which DWA analyses with different in-medium interactions can lead to contradictory conclusions about the underlying nuclear structure.

Summarising, differential cross sections from the inelastic scattering of intermediate energy protons off ^{208}Pb have been predicted for various excited states of diverse nature. A fully microscopic parameter-free model of the reactions was used. The density matrices required in the scattering calculations (elastic and inelastic) were obtained from SCRPA model calculations made using the D1S effective interaction. Those SCRPA densities were folded with the Melbourne g-matrix interaction to produce the microscopic optical potentials from which excellent predictions of elastic scattering cross sections have been made [13]. The same structure model and effective NN interaction were used to define all elements required in a fully microscopic DWA model for inelastic scattering. Excellent agreement with cross-section data has been obtained for inelastic proton scattering leading to many final states of the target and for a number of incident energies from 65 to 201 MeV. Excitations of high spin states, up to the 12_1^+ state have also been well explained with the model and so, proton scattering has been shown to be a means to precisely investigate the structure description of heavy spherical nuclei. This goal has been achieved because no phenomenological input or arbitrary renormalisation process enters our microscopic model analyses. Only with that condition can unambiguous conclusions be drawn about the structure of target nuclei. Moreover, a disagreement is observed between SCRPA + D1S-based calculations and measurements for inelastic proton scattering in the case of the 5_1^- state revealing an overestimation of the calculated neutron transition density associated to this excitation. This is an example where proton scattering studies complement electron scattering studies [22] to pinpoint a deficiency in a description of nuclear structure. Finally, we have shown that a precise description of nuclear structure is needed to account for inelastic scattering. Calculations made using "degraded" structure information (here by omission of Y components or by use of a reduced configuration space) produce observables that do not match experimental data as well as the full ones. This highlights the crucial role played by long range correlations in the description of the structure and scattering properties of the excited states of double-closed shell nuclei.

We have applied this approach to the study of discrete excitations and giant resonances in other double-closed shell or single-closed shell nuclei for which RPA is still a good approximation. The same framework can also be extended beyond discrete excitations, into the continuum, to analyse the pre-equilibrium emission associated with incoming nucleons. Results of such studies will be reported in future papers.

Acknowledgement

This work was performed in part under the auspices of the US Department of Energy by Lawrence Livermore National Laboratory under Contract DE-AC52-07NA27344. We wish to thank J. Raynal for his help in using his DWBA code in this work.

References

[1] D. Gupta, E. Khan, Y. Blumenfeld, Nucl. Phys. A 773 (2006) 230.
[2] K. Amos, et al., Adv. Nucl. Phys. 25 (2000) 275.
[3] A. Lagoyannis, et al., Phys. Lett. B 518 (2001) 27.
[4] S. Karataglidis, et al., Phys. Rev. C 65 (2002) 044306.
[5] J. Klug, et al., Phys. Rev. C 67 (2003) 031601(R).
[6] S. Karataglidis, et al., Phys. Rev. Lett. 79 (1997) 1447.
[7] S. Karataglidis, Y.J. Kim, K. Amos, Nucl. Phys. A 793 (2007) 40.
[8] K. Amos, S. Karataglidis, Y.J. Kim, Nucl. Phys. A 762 (2005) 230.
[9] Y.J. Kim, K. Amos, S. Karataglidis, Nucl. Phys. A 779 (2006) 82.
[10] K. Amos, A. Faessler, V. Rodin, Phys. Rev. C 76 (2007) 014604.
[11] J.P. Blaizot, D. Gogny, Nucl. Phys. A 284 (1977) 429.
[12] J.F. Berger, M. Girod, D. Gogny, Comput. Phys. Commun. 63 (1991) 365.
[13] M. Dupuis, S. Karataglidis, E. Bauge, J.-P. Delaroche, D. Gogny, Phys. Rev. C 73 (2006) 014605.
[14] E. Becheva, et al., Phys. Rev. Lett. 96 (2006) 012501.
[15] J.P. Jeukenne, A. Lejeune, C. Mahaux, Phys. Rep. 25 (1976) 83.
[16] Y. Fujita, et al., Phys. Rev. C 40 (1989) 1595.
[17] S. Kailas, Phys. Rev. C 35 (1987) 2324.
[18] G.S. Adams, et al., Phys. Lett. B 91 (1980) 23.
[19] V. Comparat, et al., Nucl. Phys. A 221 (1974) 403.
[20] A. Ingemarsson, B. Fagerstrom, Phys. Scr. 13 (1976) 208.
[21] M.A. Hofstee, et al., Nucl. Phys. A 588 (1995) 729.
[22] J. Heisenberg, et al., Phys. Rev. C 25 (1982) 2292.
[23] V.E. Starodubsky, N. Hintz, J. Phys. G 21 (1995) 803.
[24] Y. Fujita, et al., Phys. Lett. B 91 (1980) 27.
[25] Y. Fujita, et al., Phys. Lett. B 247 (1990) 219.
[26] N. Anantaraman, H. Toki, G.F. Bertsch, Nucl. Phys. A 398 (1983) 269.